

It can be seen that the minimum mass will be obtained when $\langle \Sigma S_i \rangle$ is a maximum. This will occur when the structure is under maximum isotropic tensile stress S_0 , that is, when $S_1 = S_2 = S_3 = S_0$, provided that S_0 is not much less than S_y . It follows then that

$$m_{st} \geq \frac{1}{8} \rho_{st} E_{mag}/S_0 \quad (15)$$

This minimum may be difficult to achieve for any practical coil design. It perhaps may be approached in a coil design that produces a quadrupole-like field at a large distance, but such a coil does not appear attractive for shielding purposes.

The minimum mass for a structure consisting of thin plates or shells will occur when each section is under maximum biaxial tensile stress, that is, when each principal stress in the plane of the shell equals S_y , and the stress normal to the shell may be neglected. In this case, one has

$$m_{st} \geq \frac{1}{2} \rho_{st} E_{mag}/S_y \quad (16)$$

The minimum in (16) is approached for a very flat (or single-turn) solenoid supported by the disk-like structure. In this example, the mass is mostly in the disks, which are under tensile stress S_y in both the radial and azimuthal directions.

In a previous result presented by Levy,⁵ a minimum mass twice that of (16) was obtained by assuming that in any element of volume each principal stress is supported by an individual structural element. The possibility of a structural member bearing more than one stress, in particular, more than one tensile stress, apparently was not considered.

The ratio of the structural mass to $\rho_{st} E_{mag}/S_y$ is shown in Fig. 3 for the single-cylinder and disk-cylinder structures. In accordance with (14), as L/R approaches zero the ratios approach unity and $\frac{1}{2}$, respectively. The increase in these ratios with increasing L/R can be attributed to the additional mass required to support the compressive force F_z . The lower mass of the disk-cylinder combination results from the replacement of some of the single tensile-stressed material in the single-cylinder by double tensile-stressed material in the disks. If, instead of the disks, (single tensile-stressed) spokes had been used, no mass savings would have been realized. The mass savings obtained by replacing uniaxially stressed structural elements (e.g., spokes or rings) with biaxially stressed elements (e.g., disks or cones) may be useful in other applications.

Concluding Comments

With the decrease in structural mass gained by using biaxially stressed structural elements, additional savings in the overall mass by reducing the amount of superconducting wire used or by reducing the mass of the cryogenic components becomes more important. The development of improved structural materials will enhance the magnetic shield concept further.

To complete the design of a magnetic shield, more detailed information concerning the variation of the shielded volume with coil shape and magnetic moment is required.

References

- ¹ Levy, R. H., "Radiation shielding of space vehicles by means of superconducting coils," *ARS J.* **31**, 1568-1570 (1961).
- ² Brown, G. V., "Magnetic radiation shielding," *Proceedings of the International Conference on High Magnetic Fields* (M.I.T. Press and John Wiley & Sons Inc., New York, 1962), pp. 370-378.
- ³ Tooper, R. F., "Electromagnetic shielding feasibility study," Armour Research Foundation Rept. 1196-10 (January 1963).
- ⁴ Nádai, A., *Plasticity* (McGraw-Hill Book Co. Inc., New York, 1931), Chap. 27, p. 182.
- ⁵ Levy, R. H., "Author's reply to Willinski's comment on 'Radiation shielding of space vehicles by means of superconducting coils,'" *ARS J.* **32**, 787 (1962).

Experimental Unsteady Airfoil Lift and Moment Coefficients for Low Values of Reduced Velocity

H. NORMAN ABRAMSON* AND GUIDO E. RANSLEBEN JR.†
Southwest Research Institute, San Antonio, Tex.

A SOMEWHAT open question of long standing relates to the accuracy of the classical aerodynamic theory for oscillations of a two-dimensional airfoil at low values of reduced velocity or, alternatively, at high values of reduced frequency, k . The situation has been summarized by Bisplinghoff et al.,¹ noting the difficulties encountered by various investigators in obtaining experimental data for $1/k < 2.0$, and particularly for $1/k < 1.0$. The various experimental data show generally excellent agreement with theory at high values of reduced velocity ($1/k > 2.5$), except for the lift and moment due to pitching; however, at lower values of reduced velocity ($0.8 < 1/k < 2.0$) several of the coefficients show increasingly poor agreement between theory and experiment.

Interest in this question has been maintained over a number of years not only for its intrinsic importance in the development of unsteady aerodynamic theory, but because a steady increase in available data on flutter of foils in dense media, more typical of hydrofoil boat applications, has revealed the apparent existence of serious discrepancies between calculated and measured flutter speeds.² Because of the low values of reduced velocity generally involved, some controversy has developed as to the nature of these discrepancies and the implications regarding the classical theory; recent theoretical and experimental studies³ have not clarified the picture. An effective answer to this problem probably will depend primarily upon the availability of fundamental experimental data on the unsteady aerodynamic coefficients.

The authors presently are engaged in a study of hydroelastic characteristics of submerged lifting surfaces for hydrofoil applications and have acquired experimental data on oscillatory lift and moment distributions on a rectangular cantilever foil of aspect ratio 5 in water under fully wetted flow conditions.⁴ These data at a low reduced velocity are of such nature that they may be correlated directly with similar data obtained during wind-tunnel tests at higher reduced velocities,⁵ at essentially the same Reynolds numbers. Almost identical experimental techniques and procedures were employed in both programs.

Figures 1-4 present plots of the oscillatory lift and moment coefficients due to bending and torsion. In each figure, experimental data from both wind-tunnel and water-towing tank tests at 50% semispan are compared with the classical two-dimensional theory. The coefficients are given in terms of magnitude and phase angle vs reduced velocity, $1/k$, where the following notation applies:

- L_{hb} = nondimensional oscillatory lift coefficient due to bending, positive downward = L_h
 L_{ha} = nondimensional oscillatory lift coefficient due to torsion about the quarter-chord, positive downward = L_a

Received March 11, 1963. The results presented in this paper were obtained during the course of research conducted under Contract Nonr-3335(00), BuShips Fundamental Hydromechanics Research Program, administered by the David Taylor Model Basin.

* Director, Department of Mechanical Sciences. Associate Fellow Member AIAA.

† Senior Research Engineer, Department of Mechanical Sciences. Member AIAA.

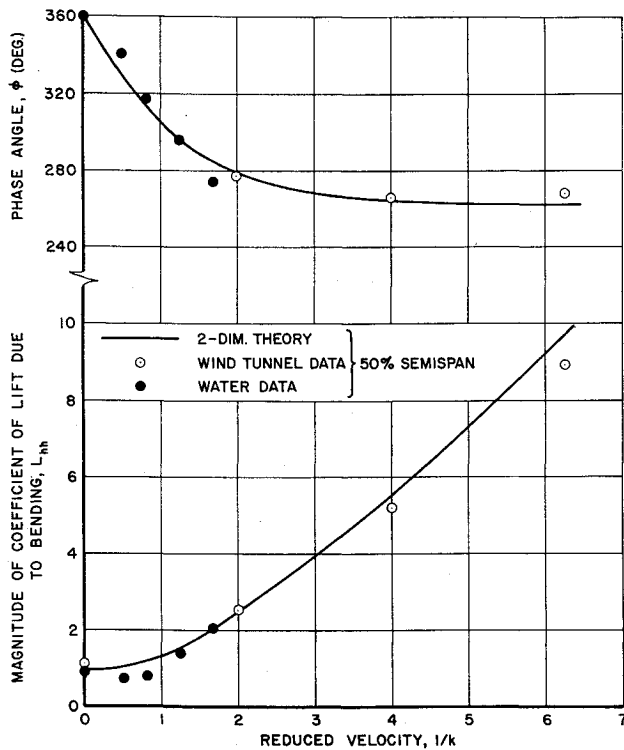


Fig. 1 Unsteady lift coefficient due to bending

$M_{\alpha h}$ = nondimensional oscillatory moment coefficient about the 31% chord due to bending, positive for forcing leading edge upward = $M_h - (d/b)L_h$
 $M_{\alpha\alpha}$ = nondimensional oscillatory moment coefficient about the 31% chord due to torsion about the quarter-chord, positive for forcing leading edge upward = $M_\alpha - (d/b)L_\alpha$
 b = semichord, ft
 d = distance from quarter-chord to moment axis, positive aft, ft

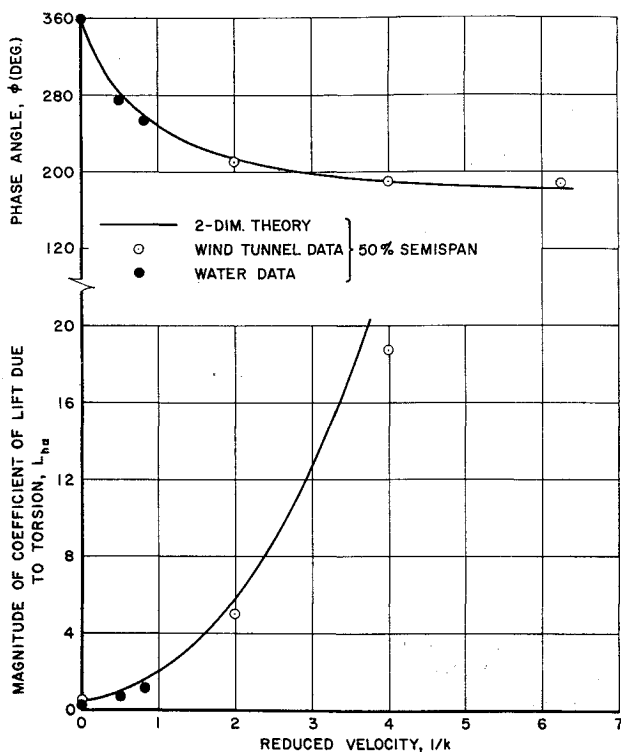


Fig. 2 Unsteady lift coefficient due to torsion about 25% chord

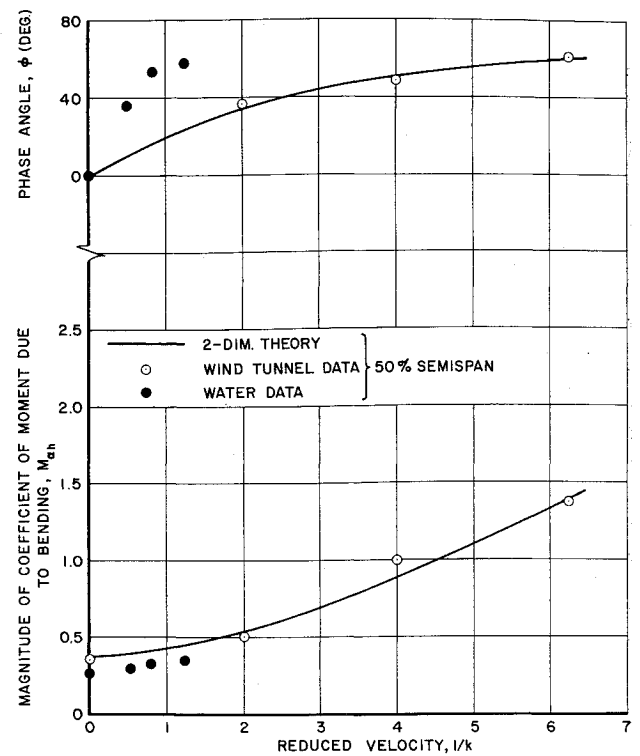


Fig. 3 Unsteady moment coefficient about 31% chord due to bending

k = "reduced" frequency, nondimensional = $b\omega/V$
 V = velocity, ft/sec
 ω = excitation frequency, rad/sec

and L_h , L_α , M_h , and M_α are the conventional quarter-chord coefficients.

The wind-tunnel data were taken for torsion and moment axes about the 35% chord and therefore had to be transformed for direct comparison with the towing-tank data, as given in the figures.

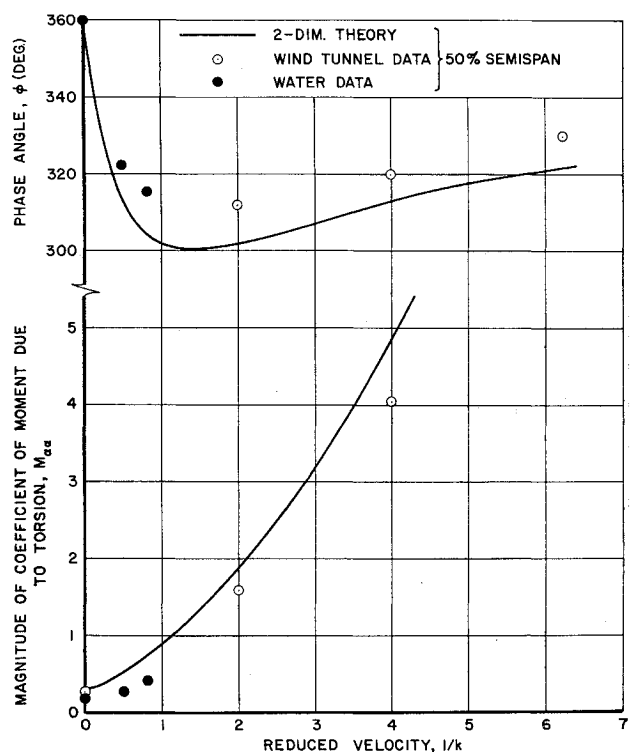


Fig. 4 Unsteady moment coefficient about 31% chord due to torsion about 25% chord

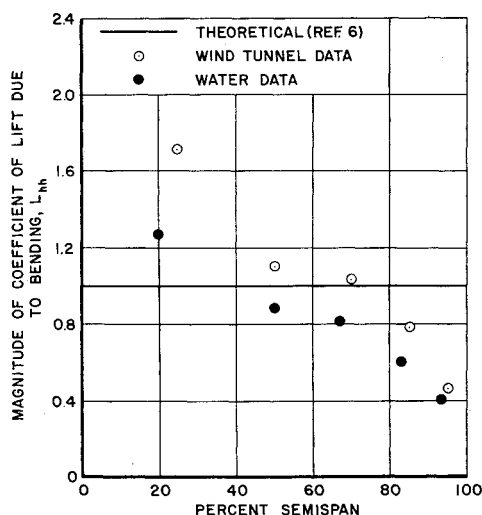


Fig. 5 Lift coefficient due to bending ($1/k = 0$)

Although the data from the tests in water are not of as high quality as from those in air, correlation between the two sets of experimental data is remarkably good, with the exception of the phase angle of moment due to bending (Fig. 3). Agreement between experimental and theoretical lift coefficients is generally good, but that between experimental and theoretical moment coefficients leaves something to be desired. The phase of the moment due to bending (Fig. 3) is puzzling because this is the only instance where the air and water-test data do not appear to correlate well; one could speculate that the experimental data *do* correlate and that any deviation resides with the theory (compare with the phase variation shown in Fig. 4). The moment due to torsion is interesting because the two sets of experimental data correlate very well but differ significantly from theory; for the higher values of reduced velocity, this seems to agree generally with previous investigators. It is emphasized that the selection of 50% semispan as a reference station was entirely arbitrary, dictated only by the fact that this was the only spanwise station at which measurements were made in both air and water tests.

Figure 5 shows that the general effect of the actual finite span on the shape of the spanwise distribution remains significant down to even $1/k = 0$ (the other coefficients show quite similar effects). Of course, theoretical finite span effects⁶ begin to diminish rapidly for small values of reduced velocity, reducing to the two-dimensional values of lift and moment at $1/k = 0$. More detailed comparisons with finite span theory over the range of reduced velocities are given elsewhere.⁴

Although few final conclusions should be drawn from the limited data on hand and the few correlations with theory that have been made, the extent of the differences between the classical theory and the measured coefficients at low reduced velocities appears to be significant. This applies particularly to the moment coefficients, where the phase of the moment due to bending requires additional data, and both the magnitude and phase of the moment due to torsion depart from theory rather significantly, on a percentage basis, as reduced velocity decreases.

References

- ¹ Bisplinghoff, R. L., Ashley, H., and Halfman, R. L., *Aeroelasticity* (Addison-Wesley Publishing Co., Cambridge, Mass., 1955), pp. 280-281.
- ² Abramson, H. N. and Chu, W. H., "A discussion of the flutter of submerged hydrofoils," *J. Ship Res.* **3**, 5-13 (October 1959).
- ³ Various papers presented at the Fourth Symposium on Naval Hydrodynamics, Washington, D. C., Office of Naval Research ACR-73 (August 27-31, 1962).
- ⁴ Ransleben, G. E., Jr. and Abramson, H. N., "Experimental

determination of oscillatory lift and moment distributions on fully submerged flexible hydrofoils," TR 2, Contract Nonr-3335(00), Southwest Res. Inst. (November 1962).

⁵ Epperson, T. B., Pengelley, C. D., Ransleben, G. E., Jr., Wilson, L. E., and Younger, D. G., Jr., "Nonstationary airload distributions on a straight flexible wing oscillating in a subsonic wind stream," Wright Air Dev. TR 55-323 (January 1956).

⁶ Reissner, E. and Stevens, J. E., "Effect of finite span on the airload distributions for oscillating wings. II.—Methods of calculation and examples of application," NACA TN 1195 (October 1947).

Turbulent Mixing of Compressible Free Jets

R. C. MAYDEW* AND J. F. REED†

Sandia Corporation, Albuquerque, N. Mex.

THE effect of Mach number on the spreading rate of turbulent free jets (in the half-jet mixing region) is not clearly defined. Estimates^{1,2} of σ , jet-spreading parameter, as a function of Mach number differ by a factor of 2 at $M = 2$.

An experimental investigation³ of the turbulent mixing of axisymmetric jets with quiescent air at nozzle exit Mach numbers of 0.70, 0.85, 0.95, 1.49, and 1.96 was conducted at Sandia Laboratory. Radial Pitot and static pressure surveys were made at 0.5, 1.0, 2.0, 3.0, and 3.84 nozzle diameters downstream of the 3-in.-diam nozzles. The 0.042-in.-diam Pitot and static probes were mounted on a lathe bed assembly. Probe position was measured with a 10-turn Helipot geared to the lathe bed assembly. Probe position and pressure data, measured by unbonded strain-gage transducers, were recorded in both analog (strip chart recorders) and digital (IBM cards) form. Data reduction with the CDC 1604 high-speed computer greatly facilitated handling the copious quantity of data.

Velocity profiles were calculated, assuming a constant total temperature through the mixing region. The virtual origin of the mixing region (resulting from the nozzle-wall boundary layer) was determined by extrapolating the width of the mixing region $b_{0.1}$ (for the five axial stations) to zero. The width $b_{0.1}$ is defined as the radial distance between 0.1 $(V/V_1)^2$ and 0.9 $(V/V_1)^2$ streamlines, where V/V_1 is the ratio of local velocity to velocity at the inner edge of the mixing region. The measured virtual origins are 0.2, 0.5, and 0.8 in. upstream of the nozzle exit for Mach 0.70, 0.85, 0.95; 1.49; and 1.96; respectively. The data indicated linear growth of the mixing region with axial distance.

The experimental velocity distributions (in the nondimensional form of $\sigma y/x_e$ vs V/V_1) were compared with Crane's⁴ and the error-function theoretical profiles. The jet-spreading parameter, σ , is proportional to the spreading rate of the mixing region and is determined by comparison of experimental with theoretical profiles. The coordinates y and x_e are the radial and the axial-plus-virtual-origin dimensions, respectively, with y measured from the $V/V_1 = 0.5$ streamline. Considerable effort was devoted to trying to fit the data (by the right choice of σ) to the error function distribution, since this simple mathematical model is easier to apply to other problems. However, the data correlated well with Crane's⁴ (or Gortler's⁵) solution for incompressible flow. The correlation is shown in Fig. 1 for $\sigma = 10.5, 10.8, 11.0, 15.0$, and 20.0 for Mach 0.70, 0.85, 0.95, 1.49, and 1.96, respectively. Data from 16 repeat runs³ (not presented herein)

Received March 11, 1963.

* Supervisor, Experimental Aerodynamics Division. Associate Fellow Member AIAA.

† Supervisor, Facilities Section. Member AIAA.